

We are IntechOpen, the world's leading publisher of Open Access books Built by scientists, for scientists

6,900

Open access books available

185,000

International authors and editors

200M

Downloads

Our authors are among the

154

Countries delivered to

TOP 1%

most cited scientists

12.2%

Contributors from top 500 universities



WEB OF SCIENCE™

Selection of our books indexed in the Book Citation Index
in Web of Science™ Core Collection (BKCI)

Interested in publishing with us?
Contact book.department@intechopen.com

Numbers displayed above are based on latest data collected.
For more information visit www.intechopen.com



Investigation of Hypersonic Conic Flows Generated by Magnetoplasma Light-Gas Gun Equipped with Laval Nozzle

Pavel P. Khramtsov

Abstract

This chapter introduces new approach of hypersonic flow generation and experimental study of hypersonic flows over cones with half-angles $\tau_1 = 3^\circ$ and $\tau_2 = 12^\circ$. Mach number of the incident flow was $M_1 = 18$. Visualization of the flow structure was made by the schlieren method. Straight Foucault knife was located in the focal plane of the receiving part of a shadow device. Registration of shadow patterns was carried out using high-speed camera Photron Fastcam (300 000 fps) with an exposure time of $1 \mu\text{s}$. The Mach number on the cone was calculated from inclination angle of shock wave in the shadowgraph.

Keywords: hypersonic conic flows, light-gas magnetoplasma launcher, photometric shadow method

1. Introduction

Currently, light-gas cannons are one of the most effective devices for accelerating shells of relatively large mass to speeds comparable to the orbital. In this area of research, intensive and extensive experimental work is being carried out to study high-speed impact, resistance of materials to high-speed action of solid particles, hypersonic flows around axisymmetric bodies and are closely related to the development of aviation and space technology. In this case, some types of guns with the replacement of the accelerating channel by the Laval nozzle can be effectively used to study hypersonic flows around bodies, since the parameters of the working gas required for high-speed throwing and generation of a hypersonic air flow are identical. High-speed throwing system parameters and technical requirements are described in [1–5]. Since the 40s of the 20th century the generation of hypersonic flows, development of measurement methods and study of such flows structure over various test bodies were carried out by researchers from all over the world [6–16]. Numerical modeling methods mentioned, for example in [10, 11, 17–19], were added to the experimental tools of the research with the development of computer technology. However, it should be noted that experimental studies of hypersonic flows around the objects are still preferred. Due to the importance of problems to be solved flight tests are often used for higher authenticity of the experimental data. Usually total and static pressure is measured by means of Pitot-Prandtl probe to determine

the Mach number, but in large number of research works measurements are not carried out due to complicated experimental techniques. Researchers [6, 7, 11–16] used the initial Mach number calculated from Laval nozzle geometrical parameters. Pressure measurement using a Pitot-Prandtl probe and temperature measurement using a thermocouple significantly distort the flow structure, complicate the design due to the need to place measuring elements inside and on the surface of the models under study, which, in the absence of flow visualization, can introduce uncontrollable errors in the experimental results. In hypersonic aerodynamic facilities preferable methods of research are optical methods with high-speed cameras as the registering devices. Methods of optical visualization of supersonic flows include a method of a laser knife, smoke visualization, visualization by means of the spark discharge, etc. [13, 15, 16, 18]. Optical methods based on the relationship between the optical and thermodynamic properties of the medium (shadow methods, interference methods, spectral diagnostics) allow measurements in hypersonic flows with high accuracy. In some cases, to visualize and measure the temperature field on the surface of the model, a thermosensitive coating is used as an alternative to measurements using thermocouples [8, 9]. Research in the field of high-speed impact and diagnostics of hypersonic flow are often interrelated tasks, which makes it necessary to create experimental installations equipped with systems for optical visualization and diagnostics of the flow and measurement of the Mach number, which makes it possible to study hypersonic flow around objects without suppressing the investigated gas flow.

2. Experimental equipment for hypersonic flow generation and optical diagnostics

In most cases, to implement a hypersonic gas flow with a high Mach number, a shock tube equipped at the end with a diaphragm and a Laval nozzle is used [18–20]. In this case, the hot gas behind the front of the reflected shock wave flows out through the nozzle into the vacuum reservoir at a hypersonic speed. However, due to the large expansion of the gas, its density turns out to be rather low, which greatly complicates the visualization of the flow. Thus, it is possible to estimate the angles of deflection ε_x and ε_y of the probe light beam in geometrical optics approach while schlieren method of hypersonic flow visualization is used [21].

$$\varepsilon_x = \frac{1}{n_0} \int \frac{\partial n(x, y)}{\partial x} dz; \quad \varepsilon_y = \frac{1}{n_0} \int \frac{\partial n(x, y)}{\partial y} dz. \quad (1)$$

At the same time gradients of gas refraction index $\frac{\partial n(x, y)}{\partial y}$ and $\frac{\partial n(x, y)}{\partial x}$ are very small when the light gas outflows into vacuum. If helium is used as a light gas and the residual pressure in the vacuum chamber is 1 Torr and the characteristic scale of the streamlined body is $\sim 10^{-2}$ m, then the characteristic gradients of the refractive index do not exceed $5 \times 10^{-6} \text{ m}^{-1}$. Under these conditions, the use of shadow methods and interference diagnosis becomes almost impossible. Therefore, in such cases, it is necessary to use the methods of multipass interferometry, multibeam interferometry, interferometry in polarized light, holographic methods or shadow methods with a large focal length and special imaging diaphragms [22]. On the other hand, the use of light-gas launcher where accelerating channel is replaced with Laval nozzle allows to receive a hypersonic flow with high optical density and to apply Tepler method to its visualization. Hypersonic flow facility studied in this research is a modified light-gas launcher we used for ballistic tests and described in details in article [23]. The scheme of the experimental setup is shown in **Figure 1**.

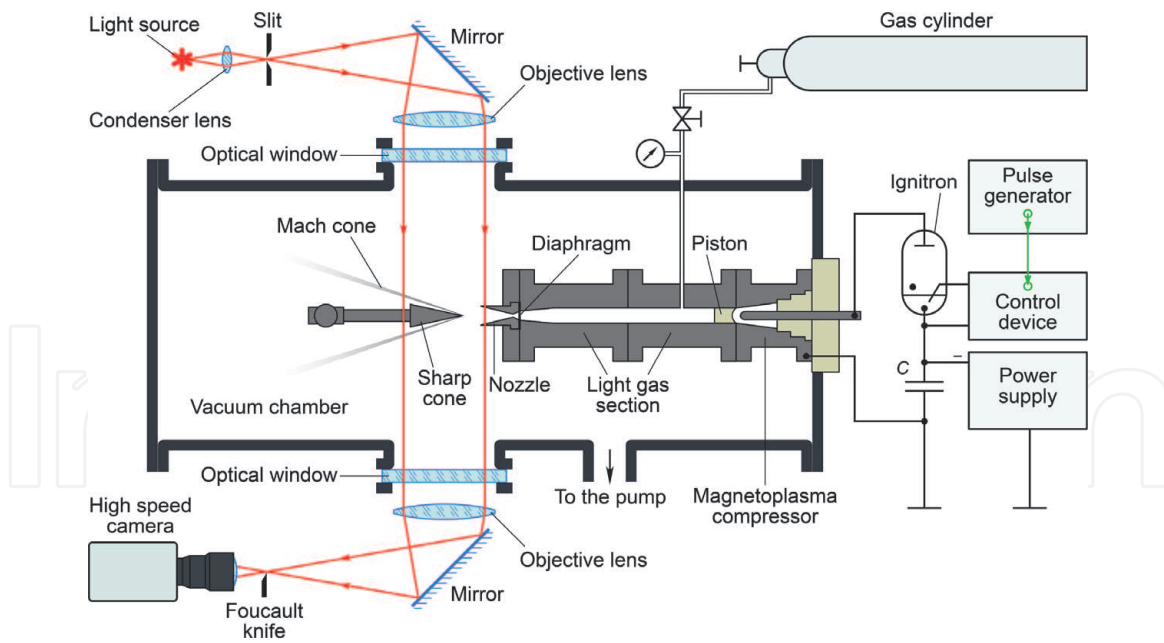


Figure 1.
 Scheme of experimental facility.

This light-gas gun allows to accelerate balls with a diameter of 2.5 mm to 4 mm made of high-alloy steel to speeds of 2.5–4 km/s.

During the experiments, the light gas section was filled with helium to a pressure of 40 bar. Experiments on hypersonic flow around cones were carried out in a vacuum chamber with a residual gas pressure of 1 Torr. As a result of a high-current discharge in a magnetoplasma accelerator filled with gunpowder, the piston is set in motion and causes an adiabatic compression of the light gas. The capacitor bank of 1 200 μF was charged to the voltage 4.5 kV. In front of the confuser of Laval nozzle 5 brass diaphragms 100 μm thick each were placed. The rupture of diaphragms occurred when pressure in light-gas section reaches $\sim 1\,600$ bars. Compression rate and temperature of working gas can be calculated from the Poisson equation:

$$\frac{T_2}{T_1} = \left(\frac{V_1}{V_2}\right)^{\gamma-1} = \left(\frac{P_2}{P_1}\right)^{\frac{\gamma-1}{\gamma}}, \quad (2)$$

where T is gas temperature, V is gas volume, P is gas pressure and $\gamma = \frac{5}{3}$ for the monoatomic gas. Subscript 1 corresponds to initial state of gas and subscript 2 is for state of gas at diaphragms rupture. When diaphragms rupture compression rate of the working gas is about 10 and temperature is about 1500 K. With the simultaneous outflow of gas through the critical section of the Laval nozzle, further compression of the gas continues until the piston reaches the end point. The maximum compression ratio is about 50 and can be calculated as the ratio of the volume of the light gas section to the volume of the confuser of the Laval nozzle. The ratio of the throat to the outlet of the diffuser in the Laval nozzle for a Mach number of 18 was calculated using the formula [22, 24]:

$$\frac{A}{A^*} = \left(\frac{2}{\gamma+1}\right)^{\frac{\gamma+1}{2(\gamma-1)}} \frac{1}{M} \left(1 + \frac{\gamma-1}{2} M^2\right)^{\frac{\gamma+1}{2(\gamma-1)}}, \quad (3)$$

where A is area of Laval nozzle exit section and A^* is area of Laval nozzle throat. The test cones were fixed coaxially with the nozzle at a distance of 20 mm from the nozzle outlet. To visualize the hypersonic gas flow, the shadow knife-and-slit method

was used. Width of a slit was 0.16 mm. Foucault's knife was placed in the focal plane of a receiving part of the shadow device and shaded a half of the image of a slit. The 150 W halogen lamp was used as a light source. The focal length of the shadow device was 1 000 mm. Registration of shadow patterns was carried out using high-speed camera Photron Fastcam (300 000 fps) with an exposure time of $1 \mu\text{s}$ (**Figure 2**).

3. Experimental results and discussion

The analysis of shadow pictures sequence shows that at initial time the flow contains some particles formed as a result of diaphragm destruction and about each of which Mach cone (**Figure 2**) is observed. Further there is an increase of speed of a flow during $700 \mu\text{s}$ and its subsequent recession during $3\,400 \mu\text{s}$. At the maximum speed of the flow in shadow pictures the most acute angle of a shock wave inclination is observed. In **Figures 3** and **4** shadow pictures of a hypersonic flow over

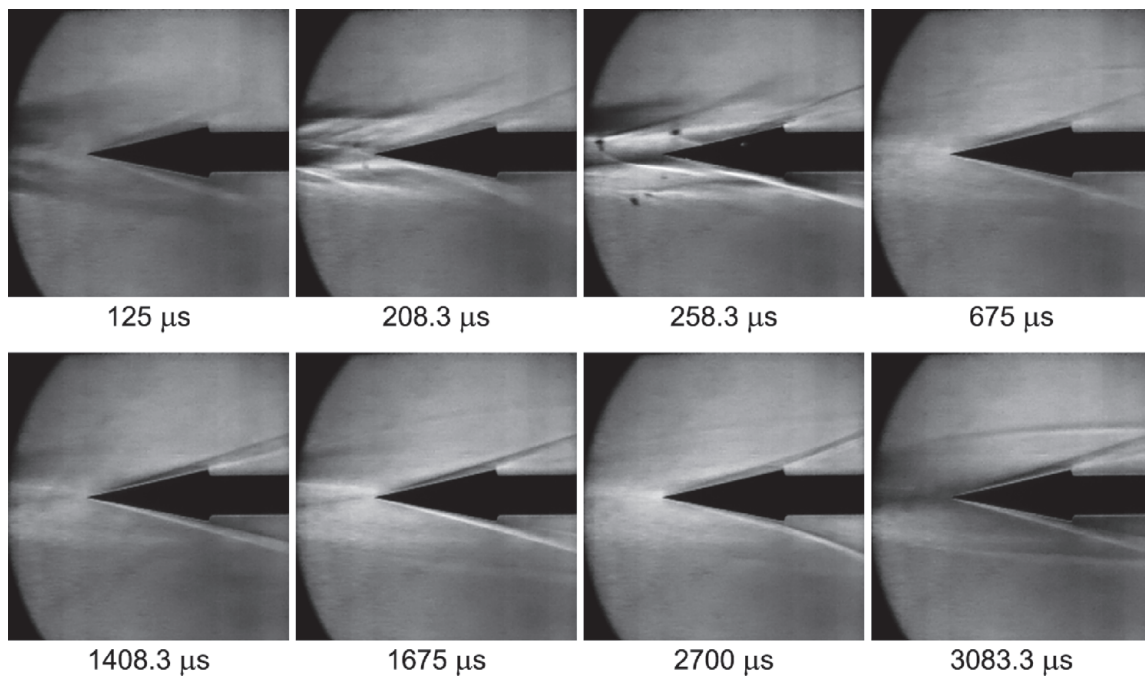


Figure 2. Shadowgraph images of a hypersonic flow over cone with half-angle $\tau_2 = 12^\circ$.

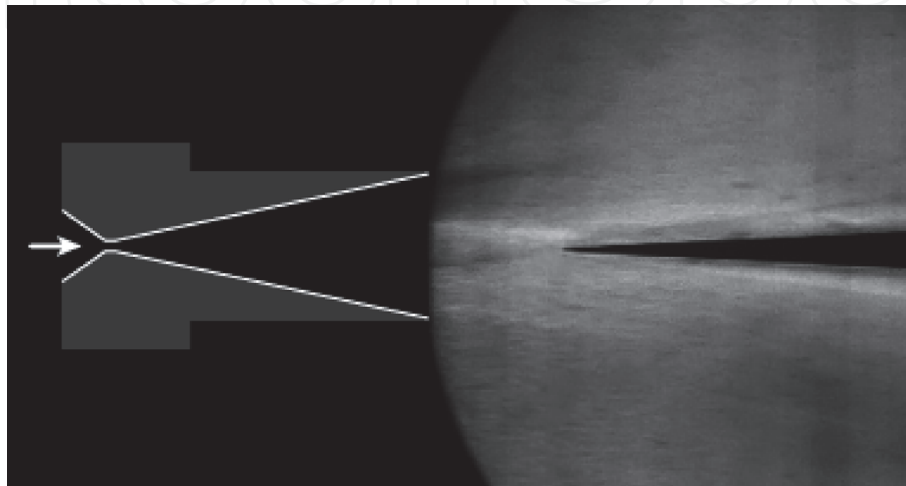


Figure 3. Shadowgraph of hypersonic flow over the cone with a half-angle $\tau_1 = 3^\circ$.

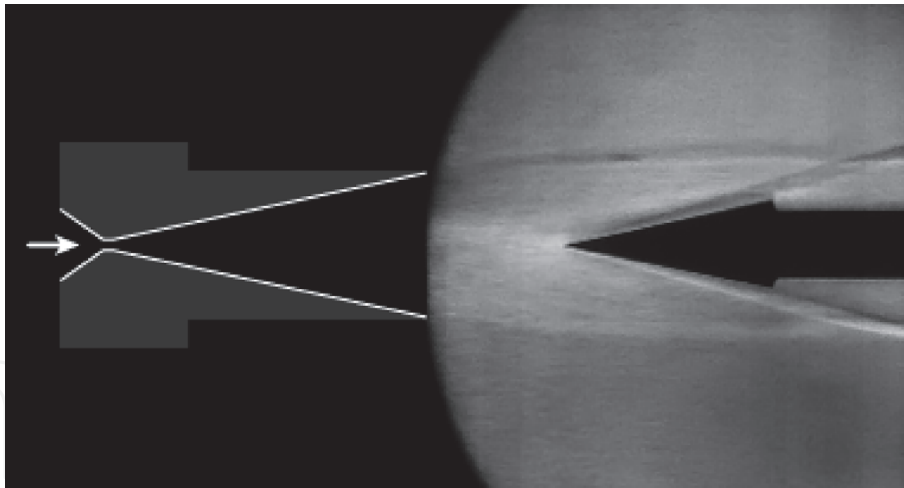


Figure 4.
 Shadowgraph of hypersonic flow over the cone with a half-angle $\tau_2 = 12^\circ$.

cones with half-angles $\tau_1 = 3^\circ$ and $\tau_2 = 12^\circ$ are presented at maximum speed of the hypersonic flow.

Correlation of Mach number and shock wave inclination angle observed on shadow images of hypersonic flow over sharp cone was described in details by [25] for the first time. Calculation of Mach number was carried out on the basis of measurement of shock wave inclination angle σ observed on shadow pictures (**Figures 3 and 4**) using formula [26]:

$$M_1 = \csc \sigma \sqrt{\frac{2(B + C - \sec \sigma)}{(\gamma + 1)\left(B + C + \frac{\cos \sigma}{\sin^2 \sigma}\right) - (\gamma - 1)(B + C - \sec \sigma)}} \quad (4)$$

where

$$B = -\ln\left(\frac{\sin \tau}{1 - \cos \tau}\right) - \frac{\cos \tau}{\sin^2 \tau}; \quad C = \ln\left(\frac{\sin \sigma}{1 - \cos \sigma}\right). \quad (5)$$

The Mach number calculation results were $M_1 = 18$ for hypersonic flow over cone with half-angle $\tau_1 = 3^\circ$ and $M_2 = 14.4$ for the cone with $\tau_2 = 12^\circ$.

4. The analysis of shadowgraphs and calculation of helium density field at a hypersonic flow over a cone

As it is known from the theory of the Schlieren technique [27], relative change of light intensity $\Delta I/I_0$ in geometrical optics approach in case of small deflection angles of the light ε is directly proportional to the magnitude of the deflection angle of the light rays in the optical inhomogeneity and can be defined by a ratio

$$\frac{\Delta I}{I_0} = \frac{\varepsilon f}{d}; \quad \Delta I = I - I_0, \quad (6)$$

where $d = 0.16$ mm is a width of a slit, $f = 1\,000$ mm is a focal length of optical system, I_0 is light intensity in the absence of an optical inhomogeneity, I is light intensity in the presence of an optical inhomogeneity. Since the streamlined body has an axial symmetry, when processing shadow pictures the assumption of

axisymmetric structure of the flow was used. The coordinate system is chosen in such a way that the x-axis is perpendicular to the edge of the imaging knife, the z-axis is directed along the probing light beam of the shadow device, and the y-axis is along the symmetry axis of the cone and the flowing stream. The origin is set at the apex of the cone. In this coordinate system, the Abel equation can be written in the form (where R is the radius of the inhomogeneity) [21, 27, 28]:

$$\varepsilon(x) = 2 \int_x^R \frac{d \ln n(r)}{dr} \frac{x dr}{\sqrt{r^2 - x^2}}. \quad (7)$$

For calculations we use Abel equation transformation where $d \ln n/dr$ is expressed explicitly:

$$\frac{d \ln n}{dr} = -\frac{1}{\pi} \frac{d}{dr} \int_r^R \frac{\varepsilon(x) dx}{\sqrt{r^2 - x^2}}. \quad (8)$$

After repeated integration [21, 27, 28] the distribution of refraction index is received:

$$\ln \frac{n(r)}{n_0} \approx \frac{n(r) - n_0}{n_0} = \frac{\Delta n}{n_0} = \frac{1}{\pi} \int_r^R \frac{\varepsilon(x) dx}{\sqrt{x^2 - r^2}}, \quad (9)$$

where n_0 is known in advance value of refraction index on the line of integration, for example in the region of undisturbed flow $n_0 = n(R) \cong 1$.

The flow area was divided into annular zones, the number of which was selected in accordance with the resolution of the video camera matrix. The deflection angle within the annular zone $[r_i; r_{i+1}]$ is assumed to be constant. Then the expression (9) can be written as a sum of elementary integrals:

$$\frac{\Delta n(r_j)}{n_0} = \frac{1}{\pi} \sum_{i=j}^{N-1} \varepsilon(r_i) \int_{r_i}^{r_{i+1}} \frac{dr}{\sqrt{r^2 - r_j^2}}. \quad (10)$$

The distribution of the refractive index in the flow is calculated as a result of independent integration at each section separately. With such processing of shadow, characteristic distortions arise in the distribution of the refractive index, which are associated with a high level of noise in the experimentally measured light intensity along the y axis. To eliminate random noise, a preliminary smoothing of the luminous intensity function along the y-axis was carried out using the least squares method [29–32]:

$$\int_{y_{min}}^{y_{max}} I''(y^2) dy \rightarrow \min. \quad (11)$$

At the same time the smoothed function values should differ from the experimental function values not more than the standard deviation δ of the probe light intensity I_0 noise. Calculation of helium density ρ was carried out with use of Gladstone-Dale Equation [21, 28].

$$n - 1 = K_{He} \rho, \quad (12)$$

where $K_{He} = 0.19607 \text{ cm}^3/\text{g}^3$ is Gladstone-Dale constant for helium. The value for the given gas and given wavelength is considered to be a constant in the wide

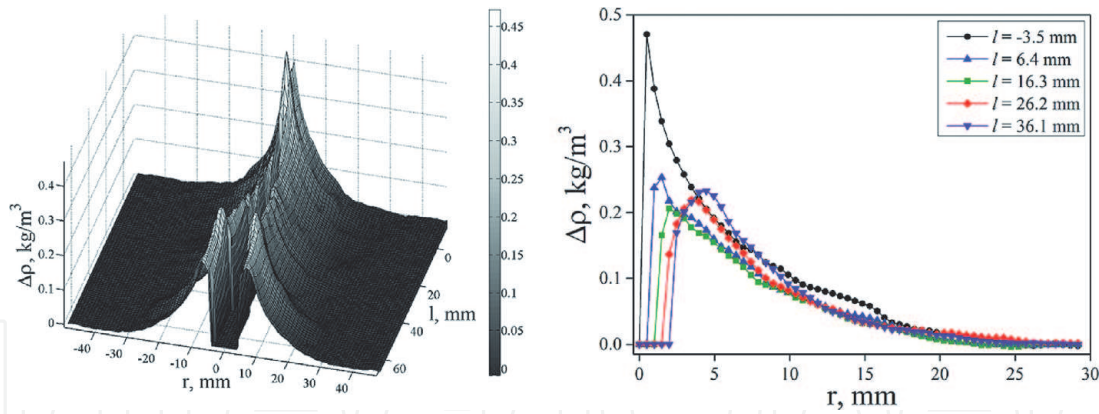


Figure 5.
 Results of density field calculations (hypersonic helium flow past cone with the half-angle $\tau_1 = 3^\circ$).

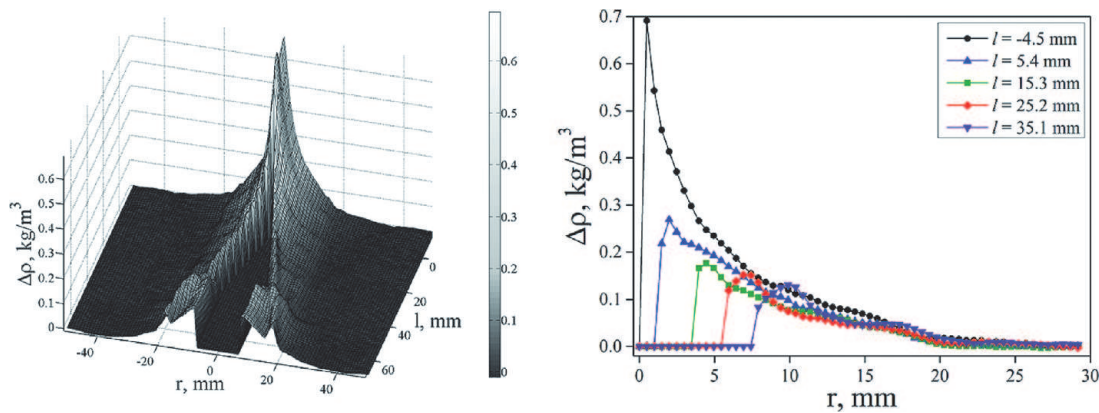


Figure 6.
 Results of density field calculations (hypersonic helium flow past cone with the half-angle $\tau_2 = 12^\circ$)

pressure range. Its value was calculated for gas under normal conditions with use of tabular values of density and refraction index [21]. As far as the initial values n_0 and ρ_0 are arbitrarily chosen values, we can calculate $\Delta\rho$ from the following equation:

$$\Delta n = K_{He} \Delta\rho. \quad (13)$$

Calculation results for helium density fields at a hypersonic flow over the cones with a half-angle $\tau_1 = 3^\circ$ and $\tau_2 = 12^\circ$ are shown in **Figures 5 and 6**.

5. Conclusions

The use of light gas ballistic systems, in which the projectile acceleration channel is replaced by a Laval nozzle, makes it possible to generate hypersonic flows with a high Mach number. The gas density of such flows is sufficient for photometric optical measurements by shadow or interference methods. This makes it possible to study hypersonic flow models of any complexity. In addition, due to the high density of the hypersonic flow, it becomes possible to experimentally study the destructive effect of the hypersonic gas flow on the bows of hypersonic missiles and aircraft.

IntechOpen

IntechOpen

Author details

Pavel P. Khramtsov

A.V. Luikov Heat and Mass Transfer Institute of the National Academy of Sciences of Belarus, Minsk, Belarus

*Address all correspondence to: drpavelpkhramtsov@gmail.com

IntechOpen

© 2021 The Author(s). Licensee IntechOpen. This chapter is distributed under the terms of the Creative Commons Attribution License (<http://creativecommons.org/licenses/by/3.0>), which permits unrestricted use, distribution, and reproduction in any medium, provided the original work is properly cited. 

References

- [1] BULAH, B. M. 1970 Nonlinear Conic Gas Flows. *Moscow Nauka* [In Russian] 343p.
- [2] GOLUBYATNIKOV, A. N. , PILYUGIN, N. N. & LEONTIEV, N. E. 2003 Methods of Upgrading the Efficiency of Light-gas Guns. *Usp. Meh.* vol. 2 (1), pp. 97–124.
- [3] SMITH, F. 1963 Theory of a Two-Stage Hypervelocity Launcher to Give Constant Driving Pressure at the Model. *J. Fluid Mech.* vol. 17 (1), pp. 113–125.
- [4] PUTZAR, R. & SCHAEFER, F. 2015 EMI's TwinGun Concept for a New Light-Gas Gun Type Hypervelocity Accelerator. *Procedia Eng.* , vol. 103, pp. 421 – 426.
- [5] PUTZAR, R. & SCHAEFER, F. 2016 Concept for a New Light-Gas Gun Type Hypervelocity Accelerator. *Int. J. Impact Eng.* **88**, 118 – 124.
- [6] ABRAMOVICH, G.N. 1973 Applied Gas Dynamics. Defense Technical Information Center. ed. 3rd.
- [7] ROGERS, E. W. E., BERRYAND, C. J. & Davis, B. M. 1971 Experiments with Cones in Low-Density Flows at Mach Numbers near 2. Her Majestys Stationery Office **3505**.
- [8] HUBNER, J. P. & CARROLL, B. F. & SCHANZE, K. S. & Ji, H. F. & HOLDEN, M. S. 2001 Temperature- and Pressure-Sensitive Paint Measurements in Short-Duration Hypersonic Flow. *AIAA J.* / vol. 39(4), 564–659.
- [9] KURITA, M. & NAKAKITA, K. & MITSUO, K. & WATANABE, S. 2006 Temperature Correction of Pressure-Sensitive Paint for Industrial Wind Tunnel Testing. *J. Aircr.* / vol. 43(5), 1499–1505.
- [10] KUSSOY, M. I. & BROWN, J. D. & BROWN, J. L. & LOCKMAN, W. K. & HORSTMAN, C. C. 1988 Fluctuations and Massive Separation in Three-Dimensional Shock-Wave/Boundary-Layer Interactions. *Tech. Rep.* 89224. NASA Tech. Mem.
- [11] BROWN, J. D. & BROWN, J. L. & KUSSOY, M. I. 1988 Fluctuations and Massive Separation in Three-dimensional Shock-Wave/Boundary-Layer Interactions. *Tech. Rep.* 101008. NASA Tech. Mem.
- [12] HORSTMANAND, C. C. & KUSSOY, M. I. 1992 Intersecting Shock-Wave/ Turbulent Boundary-Layer Interactions at Mach 8.3. *Tech. Rep.* 103909. NASA Tech. Mem.
- [13] RADZIG, A. N. 2004 Experimental Hydroaeromechanics. *Moscow MAI* [In Russian].
- [14] LEUTIN, P. G. 1976 Pressure Distribution on Sharp Cones at Angle of Sttack $\alpha \approx 10^\circ$ in Supersonic Flow. *TsAGI Sci. J.* vol. 7 (2), 163–166.
- [15] RIDYARD, H. W. 1954 The Aerodynamic Characteristics of Two Series of Lifting Bodies at Mach Number 6.86. *Tech. Rep.* L54C15. NASA Tech. Mem.
- [16] WARREN, W. R. & KAEGI, E. M. & HARRIS, C. J. & GEIGER, R. E. 1962 Shock Tunnel Studies of the Aerodynamics of Atmospheric Entry *Tech. Rep.* R62SD56. General Electric CO.
- [17] ZHIVOTNOV, S. D. & NIKOLAEV, V. S. & PROVOTVOROV, V. P. 1999 Aerodynamic Characteristics of Cones at Attack Angle Under Viscid-Nonviscid Interaction at Supersonic Velocities. *TsAGI Sci. J.* vol. 30 (3–4), 97–105.
- [18] ERDEM, E. & YANG, L. & KONTIS, K. 2009 Drag Reduction by Energy Deposition in Hypersonic Flows. In *16th AIAA/DLR/DGLR Int. Space Planes Hypersonic Syst. Technol. Conf.* 19-22 Oct., Bremen, Germany. *AIAA Paper* 2009-5347.

- [19] SARAVANAN, S. & JAGADEESH, G. & REDDY, K. P. J. 2009 Convective Heat-Transfer Rate Distributions Over a Missile Shaped Body Flying at Hypersonic Speeds. *Exp. Therm. Fluid Sci.* vol. 33 (4), 782–790.
- [20] GAYDON, A. G. & HURLE, I. R. 1963 *The Shock Tube in High Temperature Chemical Physics*. Verlag Chapman and Hall Ltd.
- [21] VASILEV, L. A. 1966 Shadow Methods. [In Russian] Nauka.
- [22] BELOZEROV, A. F. 2007 Optical Methods of Gas Flow Visualization. [In Russian] Kazan State Techn. Univ.
- [23] KHRAMTSOV, P. P. & VASETSKIY, v. A. & GRISHCHENKO, V. M. & MAKHNACH, A. I. and CHERNIK, M. YU. and SHIKH, I. A. 2015 Experimental and Analytical Study of a Two Stage Light-Gas Magnetoplasma Launcher for Ballistic Tests under Vacuum Conditions. *High Temp. Mater. Processes* vol. 19 (3–4), 209–219.
- [24] ANDERSON, J. D. 2001 *Fundamentals of Aerodynamics*. McGraw-Hill.
- [25] LIEPMANN, H. W. & ROSHKO, A. 1957 *Elements of Gas Dynamics*. John Wiley & Sons Inc.
- [26] POTTSEPP, L. 1960 Inviscid Hypersonic Flow Over Unyawed Circular Cones. *J. Aerosp. Sci.* vol. 27 (7), 558–559.
- [27] TAYLOR, H. S. and LADENBURG, R. W. 1955 *Physical Measurements in Gas Dynamics and Combustion*. Oxford University Press.
- [28] SKOTNIKOV, M. M. 1976 Qualitative Shadow Methods in Gas Dynamics. [In Russian] Nauka.
- [29] SAVITZKY, A. and GOLAY, M. J. E. 1964 Smoothing and Differentiation of Data by Simplified Least Squares Procedures. *Anal. Chem.* vol. 36 (8), 1627–1639.
- [30] STEINIER, J. & TERMONIA, Y. and DELTOUR, J. 1972 Comments on Smoothing and Differentiation of Data by Simplified Least Square Procedure. *Anal. Chem.* vol. 44 (11), 1906–1909.
- [31] BOCKASTEN, K. 1961 Transformation of Observed Radiances into Radial Distribution of the Emission of a Plasma. *J. Opt. Soc. Am.* vol. 51 (9), 943–947.
- [32] GANDER, W. and HREBICEK, J. 2004 *Solving Problems in Scientific Computing Using Maple and MATLAB*. Springer-Verlag Berlin Heidelberg.